



ISSN 1110-0451

Web site: ajnsa.journals.ekb.eg



(E S N S A)

Small Signal Analysis of Vertical Cavity Surface Emitting Lasers under the Parasitic Effect

Sh. M. Eladl and M. H. Saad

Radiation Engineering Dept. National Center for Radiation Research and Technology (NCRRT), Egyptian Atomic Energy Authority (EAEA), Cairo, Egypt

ARTICLE INFO

Article history:

Received: 17th Oct. 2021

Accepted: 16th Feb. 2022

Keywords:

Parasitic effect;

VCSEL;

Pole approximation method;

Convolution Theorem.

ABSTRACT

In this paper, a small signal analysis of a Vertical Cavity Surface Emitting Laser (VCSEL) under the parasitic condition is developed. The analysis is based on the transfer function of the considered device under the parasitic case. The dominant pole approximation scheme is used for the reduction of its characteristic equation. The Convolution Theorem is also applied to get the temporal response. All interesting parameters are outlined. The effect of parasitic cutoff frequency is also analyzed. The results show that when the parasitic cut off frequency is lower than the damping rate, the device behaves like first order low pass filter, while it behaves like second order low pass filter when the parasitic cut off frequency is greater than the damping rate. On the other side, the device operates very fast towards the second order low pass filter and up to a peak power within 1.2 ns if the resonance frequency is increased to 2 GHz, so it can be exploited in very high speed optical systems.

I. INTRODUCTION

Recently, vertical-cavity surface-emitting lasers (VCSELs) are considered new class of optical sources and have a great interest for their effective applications in optical interconnects. They are very attractive for different optical systems due to their fast response, high power, easy integration, efficient coupling, small footprint, low cost, low consumption and many other features [1]. It is necessary to reduce the parasitic effect on VCSEL to improve its performance. It is required to reduce the series resistance above the top mirror by using p-doping method. The oxide capacitance, which is considered as the largest parasitic effect, is also reduced by adding thicker layer of oxide. This will also enhance the light confinement through the structure. To reduce the pad capacitance, it is required to lower the pad dimensions itself and remove the doped layer under the pad [2-3].

The parasitic transfer function is defined as the ratio of the current through the active region of VCSEL to the applied terminal voltage and is described as a first order low pass filter function. The parasitic cutoff frequency of this low pass filter depends on the time constant formed by the pad resistance, pad capacitance, junction resistance and capacitance [4]. At high frequencies, part

of the VCSEL current is directed outside the active region due to the parasitic capacitance and limiting the VCSEL bandwidth [5].

The modulation speed of VCSEL mainly depends on the parasitic element and relaxation resonance frequency effects [6]. The parasitic element results from contact pads which introduce resistance, capacitance and inductance to the parasitic circuit. Other resistances come from the top Bragg reflectors, bottom Bragg reflectors and the active region two series parasitic capacitances come also from the oxide layer and active region [7].

In addition, the mesa capacitance results in the space charge regions within the VCSEL structure. This capacitance occurs due to the applied reverse biasing of the outer terminals of the mesa. To avoid this parasitic capacitance, a low doping at these regions leads to an increase of the depletion region and hence a decrease in its capacitance [8].

Recently, it has been shown that the input impedance is an essential factor that limits the device performance [9]. It is required to avoid the mismatch connection with the electrical driver of the VCSEL. This input impedance depends strongly on the mesa structure, oxide structures and pad size, etc. In addition, this input

impedance is temperature dependent and is affected by the ambient temperature of VCSEL. In addition, there is a parasitic inductance between the VCSEL and the driver. To reduce this parasitic effect, the VCSEL anode voltage was directly connected to the driver chip. The second solution is to put the VCSEL and driver surface at the same height [10].

In the present paper, the transfer function of VCSEL under the effect of parasitic condition is analyzed with the use of the dominant pole approximation scheme and the Convolution Theorem. The dominant pole method is applied to investigate the region of operation at different values of parasitic cutoff frequency. The Convolution Theorem is used to analyze the dynamic response of the device under consideration.

The paper outline is as follows, Section II explains the VCSEL theoretical analysis of transient response using the Convolution Theorem. In section III, the generated results are discussed using the pole approximation scheme. The conclusion and references are presented in section IV and V.

II. THEORETICAL ANALYSIS

II.1. Structure and Operation of the Device

Figure 1 shows a model of the Vertical Cavity Surface Emitting Laser (VCSEL). As shown in the figure, upper and lower Distributed Bragg Reflector (DBR) is placed above and bottom of the active region within the VCSEL structure to form upper and lower mirrors. The oxide layers, with a specific profile shape are placed to confine the injected carriers to the active region. The generated light emerges and is confined from one side of the DBR mirror with an intensive output optical power.

II.2. Dynamic Behavior

When the shunt electrical parasitic is taken into account, the dynamic transfer function can be considered as a first order low-pass filter with a parasitic cutoff frequency ω_b and the total modulated small signal response becomes a three-pole transfer function given as [11-12].

$$M(j\omega) = \frac{S(j\omega)}{I(j\omega)} = \frac{\omega_b}{j\omega + \omega_b} \frac{\omega_r^2}{\omega_r^2 - \omega^2 + j\omega\gamma} \quad (1)$$

By applying the dominant pole approximation scheme described in [13] to the above expression, one can get

$$M(j\omega) = \frac{S(j\omega)}{I(j\omega)} = \begin{cases} M_1(j\omega) = \frac{\omega_b}{j\omega + \omega_b} & \omega_b \ll \frac{\gamma}{2} \\ M_2(j\omega) = \frac{\omega_r^2}{\omega_r^2 - \omega^2 + j\omega\gamma} & \omega_b \gg \frac{\gamma}{2} \end{cases} \quad (2)$$

The transfer function in Eq. (1) has a negative real pole ω_b and another imaginary pole with a negative real part equal $\frac{\gamma}{2}$ and each pole represents the speed of response.

Where ω_r is the resonance frequency and γ is the damping frequency parameter that can be described as:

$$\omega_r = \sqrt{\frac{1}{2\pi} \frac{vg\eta_i a}{qV_m} (I - I_{th})} \quad \text{and} \quad \gamma = \frac{1}{\tau} + K\omega_r^2 \quad (3)$$

Where q is the unit charge, η_i is the injection efficiency, τ is the carrier lifetime, vg is the photon group velocity, g is the gain coefficient, V_m is the cavity volume, K is the damping factor and $(I - I_{th})$ is the above threshold injection current.

According to the dominant pole approximation scheme, when the second order pole is dominant, the transient response is written as

$$M_2(t) = \frac{2}{\omega_r} - \frac{8}{\omega_r} \frac{e^{-\frac{\gamma t}{2}} \cos\left(\frac{\sqrt{4\omega_r^2 - \gamma^2}}{2} t\right)}{4\omega_r^2 - \gamma^2} + 2 \frac{\gamma^2}{\omega_r} \frac{e^{-\frac{\gamma t}{2}} \cos\left(\frac{\sqrt{4\omega_r^2 - \gamma^2}}{2} t\right)}{4\omega_r^2 - \gamma^2} - \frac{2\gamma}{\omega_r} \frac{e^{-\frac{\gamma t}{2}} \sqrt{4\omega_r^2 - \gamma^2} \sin\left(\frac{\sqrt{4\omega_r^2 - \gamma^2}}{2} t\right)}{4\omega_r^2 - \gamma^2} \quad (4)$$

And when the first order pole is dominant, the transient response is written as

$$M_1(t) = 1 - e^{-\omega_b t} \quad (5)$$

Assuming a unit step input injection current and applying Convolution Theorem [14]

$S(t) = U(t) * M(t)$, where $*$ denotes to the convolution between $U(t)$ and $M(t)$, $U(t)$ is a unit step signal and $M(t)$ is the time domain of $M(j\omega)$

$$S(t) = I(t)U(t) * M(t) = \int_0^t U(t - \mu) * M(\mu) d\mu = \int_0^t \frac{1}{\gamma} (1 - e^{-\gamma\mu}) d\mu \quad (6)$$

Then,

$$S(t) = \frac{1}{Q} P(t) \quad (7)$$

Where

$$P(t) = \left[-\omega_r^2 \sqrt{4\omega_r^2 - \gamma^2} - \omega_b^2 \sqrt{4\omega_r^2 - \gamma^2} e^{\frac{(2\omega_b - \gamma)t}{2}} \cos\left(\frac{\sqrt{4\omega_r^2 - \gamma^2}}{2} t\right) - (\gamma^2 \omega_b + \gamma \omega_b^2 - 2 e^{-\omega_b t} \omega_b \omega_r^2) e^{\frac{(2\omega_b - \gamma)t}{2}} \sin\left(\frac{\sqrt{4\omega_r^2 - \gamma^2}}{2} t\right) \right] \quad (8)$$

And

$$Q = \left[(\omega_b^2 - \omega_{b\gamma} + \omega_r^2) (\sqrt{4\omega_r^2 - \gamma^2}) \right] \tag{9}$$

Where $I(t)U(t)$ is a unit step input current and equal unity and $U(t - \mu)$ is a delayed signal.

III. RESULTS AND DISCUSSIONS

The first set of curves shown in Fig. 2a represents the relative transient behavior of VCSEL for $\omega_b = 0.1$ GHz, $\gamma = 1$ GHz and $\omega_r = 1$ GHz. The solid line curve represents the exact three-pole response and the dotted line curve corresponds to the second order dominant pole approximation, while the dashed line curve corresponds to the first order dominant pole approximation. It is clear from the Figure that the exact three-pole response is in close with the first order dominant pole approximation response, this is because the pole of the first order $\omega_b = 0.1$ GHz is close to zero in the pole-zero map than $\gamma/2 = 0.5$ GHz as in Fig. (2b).

The second set of curves shown in Fig. (3a) represents the relative transient behavior of VCSEL for $\omega_b = 2$ GHz, $\gamma = 1$ GHz and $\omega_r = 1$ GHz. In this case, the exact three-pole response is very much like the second order dominant pole approximation response, this is because the real part of the conjugate pole which equals $\gamma/2 = 0.5$ GHz is closer to zero than $\omega_b = 4$ GHz as in the pole zero map of Fig. (3b), so the second order pole is the dominant which makes the VCSEL very similar to it.

The third set of curves shown in Fig. (4a) represents the relative transient behavior of VCSEL for $\omega_b = 0.5$ GHz, $\gamma = 1$ GHz and $\omega_r = 1$ GHz. In this case where, $\omega_b = \gamma/2$, the exact three-pole response is not similar to any one of the considered approximations because all poles are not dominant as in pole zero map of Fig. (4b).

To explain the effect of resonance frequency ω_r on the transient behavior, ω_r is varied while both ω_b and γ are kept fixed. The transient response of VCSEL for the exact response, first order approximation, and second order approximation as before at $\omega_r = 2$ GHz, $\gamma = 1$ GHz and $\omega_b = 1$ GHz is shown in Fig. (5). It is clear that the device response is very similar to the first order approximation than second order approximation. Since ω_r is greater than γ , the device exhibits an oscillation with damped behavior.

If the value of ω_r is reduced to $\omega_r = 0.6$ GHz as in Fig. (6), the device response is very similar to the second order approximation than first order approximation. In

this case ω_r is lower than γ , so the device exhibits no oscillation and behaves like first order low pass filter response.

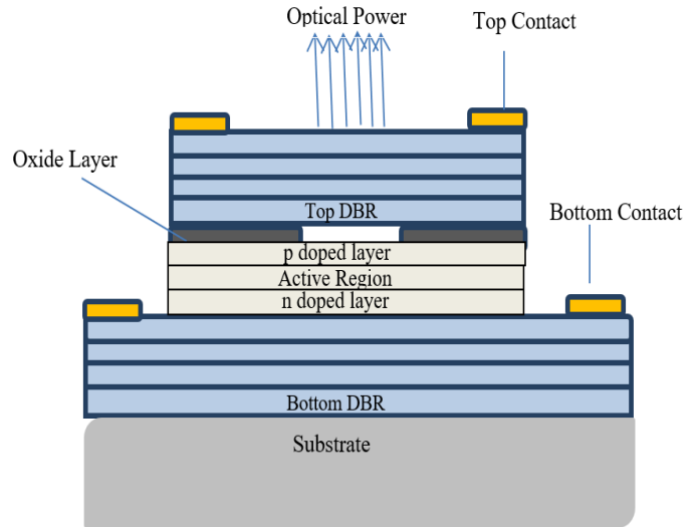


Fig. (1): Schematic structure of a Vertical Cavity Surface Emitting Laser (VCSEL)

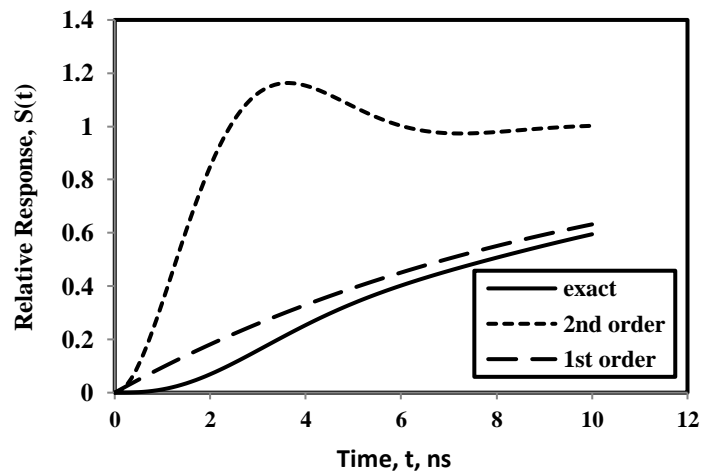


Fig. (2a): Relative transient response at $\omega_b = 0.1$ GHz for three cases, $\gamma = 1$ GHz, and $\omega_r = 1$ GHz

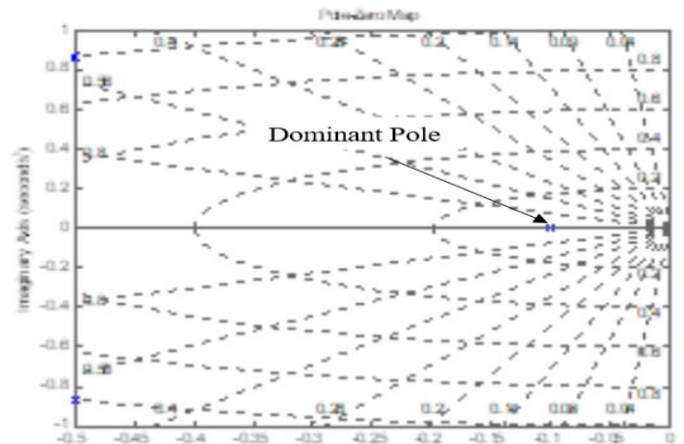


Fig. (2b): P-Z Map for $\omega_b = 0.1$ GHz , $\gamma = 1$ GHz, and $\omega_r = 1$ GHz

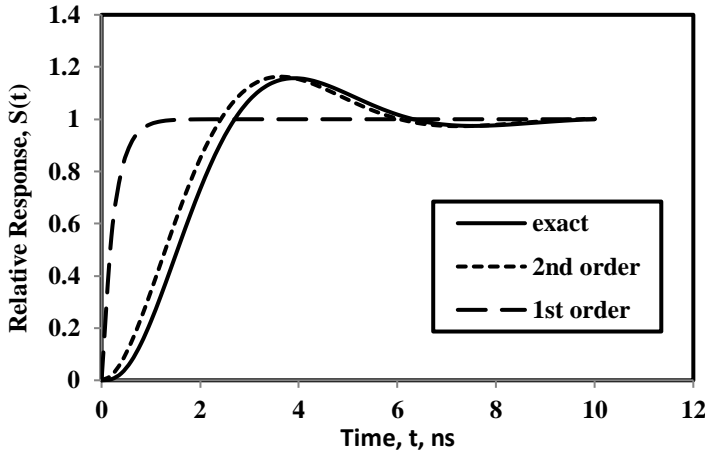


Fig. (3a): Relative transient response at $\omega_b=2$ GHz for three cases, $\gamma=1$ GHz, and $\omega_r=1$ GHz

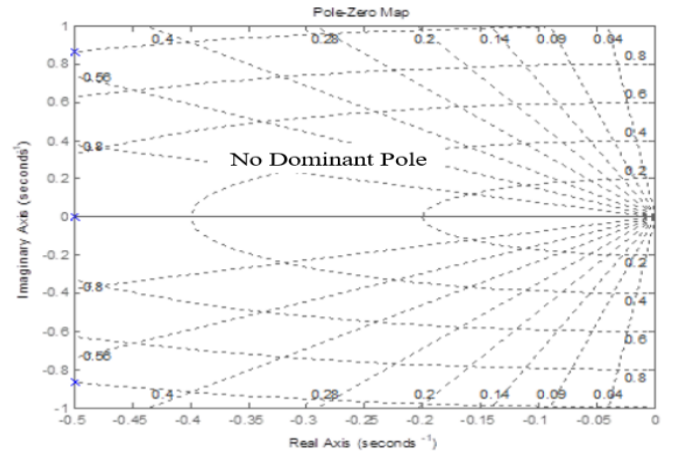


Fig. (4b): P-Z Map for $\omega_b = 0.5$ GHz , $\gamma=1$ GHz, and $\omega_r=1$ GHz

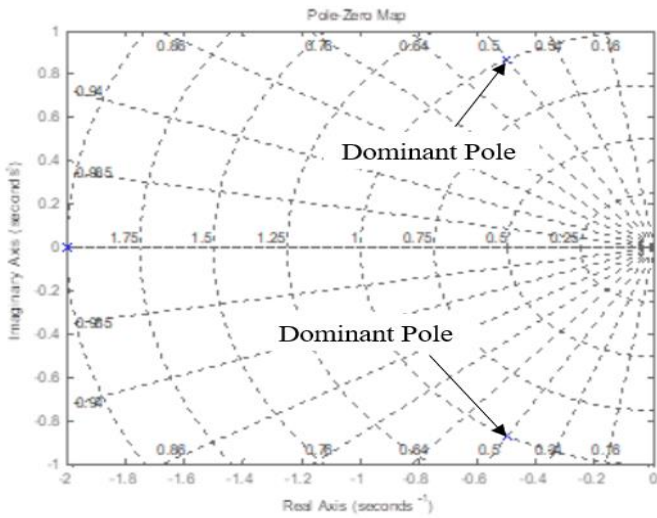


Fig. (3b): P-Z Map for $\omega_b = 2$ GHz, $\gamma=1$ GHz, and $\omega_r=1$ GHz

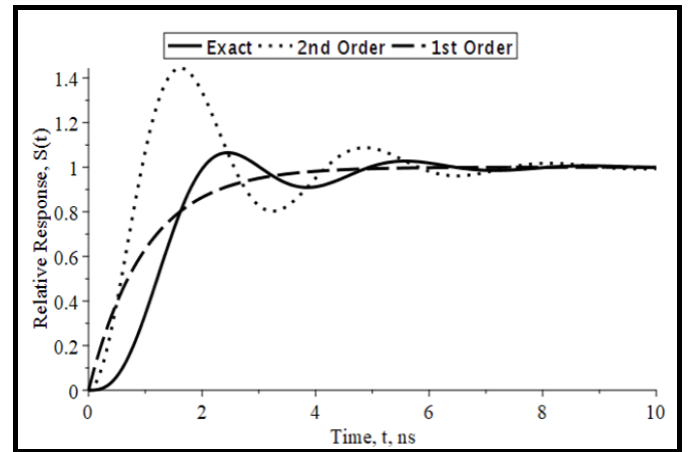


Fig. (5): Relative transient response for three cases $\omega_b=1$ GHz $\gamma=1$ GHz and $\omega_r=2$ GHz

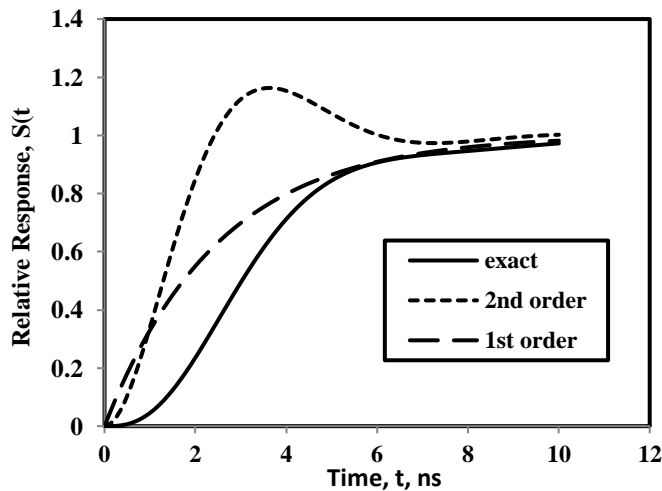


Fig. (4a): Relative transient response at $\omega_b=0.5$ GHz for three cases, $\gamma=1$ GHz, and $\omega_r=1$ GHz

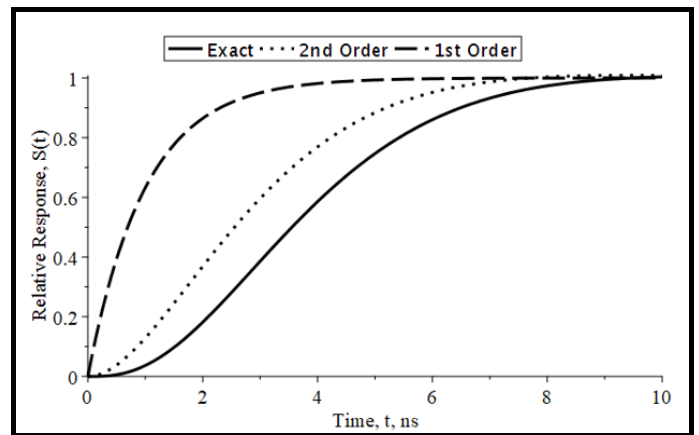


Fig. (6): Relative transient response for three cases $\omega_b=1$ GHz $\gamma=1$ GHz and $\omega_r=0.6$ GHz

IV. CONCLUSIONS

A small signal analysis based on the frequency response transfer function of a Vertical Cavity Surface Emitting Laser (VCSEL) is developed in this article. The frequency response is expressed in parasitic conditions due the layer capacitance and thermal resistance which cause additional first order low pass filter to the transfer function. The frequency damping of this parasitic case depends on the values of this resistance and capacitance. The parasitic effect in terms of its cut off frequency on the transient behavior is studied. The effect of damping rate on the dynamic behavior is also outlined. The results show that when the parasitic cutoff frequency is greater than the damping frequency, the device dynamic behavior operates like 2nd order low pass filter. Otherwise, the lower values renders the device to behave like the first order low pass filter. The effect of a rectangular pulse input signal on the device behavior is planned as a future extension to this work. This type of models can be exploited in the high speed data rate optical fiber communication systems.

V. REFERENCES

- [1] Y. Chang, C. Wang and L. Coldren, "High-efficiency, high-speed VCSELs with 35 Gbit/s error-free operation" *J. of Electronics Letters*, Vol. 43, No. 19, 2007.
- [2] A N AL-Omari et al "VCSELs with a Self-Aligned Contact and Copper-Plated Heatsink" *IEEE Photon. Technol. Lett.* Vol. 17, pp.1-9, 2005.
- [3] He xiao- Ying, et al. " High Speed Spectrum 850 nm Vertical Cavity Surface Emitting Laser (VCSEL) with BCP Planarization technique" *J. of Chinese Optics*, Vo. 11, No. 2, pp. 190-197, 2018.
- [4] Michael Muller, Werner Hofmann , Tobias Grundl, Markus Horn, Philip Wolf, Robin Daniel Nagel, Enno Ronneberg, Gerhard Bohm, Dieter Bimberg, and Markus-Christian Amann "1550-nm High-Speed Short-Cavity VCSELs" *IEEE J. of Selected Topics in Quantum Electronics*, Vol. 17, No. 5, Sept., 2011.
- [5] Mayank Raj, Manuel Monge and Azita Emami, "A Modelling and Nonlinear Equalization Technique for a 20 Gb/s 0.77 pJ/b VCSEL Transmitter in 32 nm SOI CMOS" *IEEE Journal of Solide State Circuits*, Vol. 51, No. 8, July, 2016.
- [6] A N AL-Omari et al "Fabrication, performance and parasitic parameter extraction of 850 nm high-speed vertical-cavity lasers" *J. of Semiconductor Science and Technology*, Vol. 24, 095024, pp. 1-8, 2009.
- [7] Shanglin Li , Mohammadreza Sanadgol Nezami, David Rolston and Odile Liboiron-Ladouceur "A Compact High-Efficient Equivalent Circuit Model of Multi-Quantum-Well Vertical-Cavity Surface-Emitting Lasers for High-Speed Interconnects" *Journal of Appl. Sci.*, Vol. 10, pp. 1-12., 2020.
- [8] A. M. Nadtochiy, et al. "Decreasing parasitic capacitance in vertical-cavity surface-emitting laser with selectively oxidized aperture" *Journal of Technical Physics Letters*, Vol. 38, No. 2, pp. 105-109,2012.
- [9] Alexander Grabowski, Johan Gustavsson, Zhongxia Simon He and Anders Larsson "Large-Signal Equivalent Circuit for Datacom VCSELs" *Journal of Light wave Technology*, Vol. 39, No. 10, pp. 3225-3236, 2021.
- [10] Giannis Kanakis, et al. "High-Speed VCSEL-Based Transceiver for 200 GbE Short-Reach Intra-Datacenter Optical Interconnects" *Journal of Appl. Sci.* Vo. 9, 2488, pp. 1-17,2019.
- [11] Wissam Hamad, Stefan Wanckel and Werner Hofmann "Small-Signal Analysis of Ultra-High-Speed Multi-Mode VCSELs" *IEEE Journal of Quantum Electronics*, Vol. 52, No. 7, pp. 1-12, 2016.
- [12] M. M"uller, et al. "1550-nm High-Speed Short-Cavity VCSELs" *IEEE Journal of Selected Topics in Quantum Electronics*, Vol. 17, No. 5, 2011.
- [13] Joost Rommes and Nelson Martins "Computing dominant poles of large second-order transfer functions" *Proc. Appl. Math. Mech.* 7, 2020079–2020080, 2007.
- [14] X. Zhia, D. Weib, W. Zhanga "A generalized convolution theorem for the special affine Fourier transform and its application to filtering" *International Journal for Light and Electron Optics*, Vol. 127, P. 2613–2616, 2016.